Research Square

Preprints are preliminary reports that have not undergone peer review.
They should not be considered conclusive, used to inform clinical practice,
or referenced by the media as validated information.

Dynamic Optoelectronic Assessment of Sagittal Alignment During Gait: Correlation with EOS Radiographic Parameters and Diagnostic Performance

Mourad Ould-Slimane[1]
Rouen University Hospital
Caroline Lesage[1]
Rouen University Hospital
Mathieu Lozouet[1]
Rouen University Hospital
Paul Deschamps[1]
Rouen University Hospital
Yanis Nebbache[1]
Rouen University Hospital
André Gillibert[2]
Rouen University Hospital
Nolwen Lemonnier[1]
Rouen University Hospital
François Luc[3]
fraluc.interne76@gmail.com

Rouen University Hospital

Article

Keywords: Optoelectronics, sagittal balance, spinopelvic alignment, gait analysis, postural assessment

Posted Date: September 21st, 2026

DOI: https://doi.org/10.21203/rs.3.rs-10593832/v1

License: This work is licensed under a Creative Commons Attribution 4.0 International License.
Read Full License

Additional Declarations: No competing interests reported.

Abstract

Sagittal alignment is usually assessed using static radiographs, although posture changes continuously during gait. We evaluated whether dynamic optoelectronic parameters could discriminate a controlled brace-induced sagittal perturbation and developed a graphical representation of alignment throughout the gait cycle. Thirty-five healthy male volunteers underwent EOS imaging and Vicon motion capture without and with a custom kyphosing brace. The C7-T10-S1 angle, C7'S1', and spinal angle were compared with radiographic parameters using Spearman correlations, and discrimination between conditions was quantified by the area under the receiver operating characteristic curve (AUROC). Brace application significantly altered all optoelectronic parameters (all $p < 0.0001$). C7 sagittal tilt correlated with the C7-T10-S1 angle ($r = 0.62$), C7'S1' ($r = 0.70$), and spinal angle ($r = 0.69$). AUROCs were 0.89, 0.92, and 0.94, respectively. Point-by-point graphical envelopes illustrated changes in curve shape and interparticipant variability throughout gait. Dynamic optoelectronic assessment therefore discriminated experimental sagittal perturbation and provided a continuous representation complementary to static radiography. Clinical validation in patients with spinal deformity is required.

Introduction

Sagittal spinopelvic alignment is a key determinant of standing posture, functional capacity, and health-related quality of life [1]. Sagittal malalignment, particularly anterior sagittal imbalance, is associated with pain, disability, and poorer outcomes after spinal deformity surgery [1]. Restoration of sagittal alignment has therefore become a major objective in the treatment of spinal deformity. Radiographic parameters such as pelvic incidence (PI), pelvic tilt (PT), sacral slope (SS), lumbar lordosis (LL), thoracic kyphosis (TK), and C7 sagittal tilt (C7ST) are routinely used to characterize sagittal alignment and guide treatment decisions [2–6].

Sagittal alignment is currently evaluated primarily using standing radiographs, including low-dose EOS imaging. Although these techniques provide accurate anatomical measurements, they capture only a static representation of a dynamic biomechanical system [5]. During gait, sagittal posture is continuously modulated by compensatory mechanisms involving the spine, pelvis, and lower limbs. Studies in patients with spinal deformity have shown that compensatory strategies during walking may differ substantially from those observed during static standing [7–10]. Dynamic assessment may therefore provide clinically relevant information that cannot be obtained from conventional radiographic analysis alone [5, 11].

Optoelectronic motion capture systems enable continuous analysis of spinal and pelvic motion during gait by tracking reflective markers placed on anatomical landmarks. Previous work demonstrated the feasibility of detecting experimentally induced sagittal imbalance using optoelectronic motion capture and reported significant correlations between dynamic and radiographic measurements [12]. However, the diagnostic performance of these dynamic parameters and their evolution throughout the gait cycle

have not been investigated. It therefore remains unclear which parameters most accurately identify sagittal imbalance and how sagittal alignment changes continuously during walking.

We hypothesized that dynamic optoelectronic parameters would accurately detect sagittal imbalance and correlate with standard radiographic measurements. The primary objective was to determine the diagnostic performance of these parameters for identifying sagittal imbalance. The secondary objective was to develop a graphical method for visualizing the dynamic evolution of sagittal alignment throughout the gait cycle.

Materials and methods

This prospective, single-center comparative study was approved by the Comité de Protection des Personnes Nord-Ouest III (CPP Nord-Ouest I, Rouen, France (approval No. CPP02/017/2016)). All participants provided written informed consent before enrollment. The study was conducted in accordance with the Declaration of Helsinki and French regulations governing personal data protection. The study protocol was prospectively registered at ClinicalTrials.gov, a publicly accessible registry included in the World Health Organization International Clinical Trials Registry Platform (WHO ICTRP), on 24 May 2018 (registration no. NCT03536403), before enrolment of the first participant.

Population

Healthy male volunteers were recruited through the Clinical Investigation Center (CIC INSERM 1404, Rouen University Hospital, France). Participants were randomly selected from the CIC volunteer database. Inclusion criteria were age 20–40 years, height 165–190 cm, body mass index < 30 kg/m², corrected visual acuity ≥ 6/10, no spinal symptoms, and no neurological, vestibular, or locomotor disorder likely to affect gait. Participants with a spinal deformity on EOS imaging were excluded. To induce a reversible alteration in sagittal alignment, all participants were evaluated under two conditions: without a brace and with a kyphosing brace.

Experimental induction of sagittal imbalance

A custom thermoformed kyphosing brace was used to induce anterior sagittal imbalance. The brace was designed to increase thoracic kyphosis and forward trunk inclination while permitting comfortable ambulation. Openings at the anterior superior iliac spines (ASIS), sacrum, and thoracolumbar junction allowed placement and visualization of reflective markers. Each participant underwent radiographic and optoelectronic assessment under both experimental conditions (Fig. 1).

Radiographic assessment

Low-dose biplanar EOS radiographs (EOS Imaging, Paris, France) were obtained under both conditions (Fig. 2).

Sagittal alignment was assessed using standard spinopelvic parameters [2–6], including PI, PT, SS, LL, TK, and C7ST (Fig. 3). These measurements served as the radiographic reference parameters.

Optoelectronic gait analysis

Dynamic gait analysis was performed using a Vicon® motion capture system (Biometrics, Gometz-le-Châtel, France) comprising nine infrared cameras operating at 100 Hz. Thirty-eight reflective markers were positioned on predefined anatomical landmarks according to the standardized whole-body gait analysis protocol described by Ould-Slimane et al. [12]. Markers used specifically for sagittal alignment analysis were placed over the spinous processes of C7, T10, and S1 and over both ASIS. The same trained investigator placed all markers. Participants walked along an 8-m walkway at a self-selected comfortable speed. Five trials were recorded under each condition, yielding ten acquisitions per participant.

Definition of optoelectronic parameters

Three dynamic optoelectronic parameters were used to characterize sagittal alignment (Fig. 4).

The C7-T10-S1 angle was defined as the angle between the C7-T10 and T10-S1 segments. The spinal angle was calculated automatically by Vicon Nexus software as the angle between the thoracolumbar sagittal axis and the pelvic plane. The C7'S1' parameter corresponded to the horizontal projection of the C7-S1 vector onto the ground plane. Parameters were recorded continuously during gait and averaged across the five trials obtained under each condition.

Dynamic signal processing and graphical representation

The C7-T10-S1 angle and spinal angle were analyzed continuously during each walking trial. For each participant and condition, the five trials were synchronized and smoothed using a moving-average filter (± 0.1 s) to reduce measurement noise. Gait cycles were identified and normalized using Fourier-based phase analysis. The dominant periodic component corresponding to the walking cycle was used to align recordings and normalize cycle duration across trials. The five synchronized trials were then averaged point by point to generate a representative curve for each participant and condition. Cohort-level curves were generated by pooling individual recordings and calculating point-by-point distribution envelopes. First derivatives of the smoothed C7-T10-S1 and spinal angle curves were calculated to characterize the rate of change in sagittal alignment throughout the gait cycle. This workflow enabled graphical comparison of dynamic sagittal alignment between brace and no-brace conditions.

Statistical analysis

Radiographic and optoelectronic variables are presented as medians and interquartile ranges (IQRs). Brace and no-brace conditions were compared using the Wilcoxon signed-rank test. The ability of each

radiographic and optoelectronic parameter to discriminate experimentally induced sagittal imbalance was assessed using the area under the receiver operating characteristic curve (AUROC). Because observations were paired, confidence intervals were estimated using bias-corrected and accelerated (BCa) bootstrap resampling at the participant level [13]. Correlations between C7ST and optoelectronic parameters were assessed using Spearman correlation coefficients; confidence intervals were also estimated using participant-level BCa bootstrap resampling. Pairwise comparisons between AUROCs were not performed because the study was not powered for this analysis. All tests were two-sided, and statistical significance was set at $p < 0.05$. Analyses were performed using R version 4.0.1 (R Foundation for Statistical Computing, Vienna, Austria).

Results

Thirty-six volunteers were enrolled between December 2018 and December 2019. One participant was excluded after EOS imaging revealed previously undiagnosed asymptomatic scoliosis. The final cohort comprised 35 healthy male participants with a mean age of 29.9 ± 4.3 years. All assessments were completed successfully, and no adverse events or brace-related intolerance occurred.

Induction of sagittal imbalance

Radiographic and optoelectronic parameters are summarized in Table 1.

Table 1. Radiologic and optoelectronic parameters with and without brace.

Parameter	Without brace, median (IQR)	With brace, median (IQR)	Paired difference, median (IQR)	p value*	AUROC (95% CI)
Radiographic parameters					
Pelvic incidence (°)	49.1 (44.4-57.6)	49.1 (44.7-57.6)	0.0 (−0.1-0.1)	0.084	0.51 (0.48–0.52)
Pelvic tilt (°)	10.4 (7.5-13.7)	10.8 (8.0-14.9)	−0.1 (−1.4-3.8)	0.39	0.53 (0.45–0.60)
Sacral slope (°)	41.4 (33.7-45.7)	37.8 (34.9-44.7)	0.2 (−3.6-1.6)	0.57	0.49 (0.41–0.55)
Lumbar lordosis (°)	58.6 (55.0-69.1)	52.1 (44.2-56.8)	−7.4 (−12.8-4.4)	<0.0001	0.25 (0.17–0.32)
Thoracic kyphosis (°)	−44.8 (−50.9-37.6)	−58.6 (−63.0-54.3)	−14.5 (−17.7–−9.0)	<0.0001	0.10 (0.05–0.19)
C7 sagittal tilt (°)	−1.2 (−3.2-1.3)	14.3 (9.1-16.9)	14.8 (10.0-18.0)	<0.0001	0.99 (0.96–1.00)
Optoelectronic parameters					
C7–T10–S1 angle (°)	170.2 (165.8-172.9)	160.7 (158.7-164.1)	−7.4 (−11.2–−6.1)	<0.0001	0.89 (0.82–0.94)
C7'S1' (mm)	55.2 (40.6-82.9)	133.2 (87.8-169.5)	66.2 (42.4-94.9)	<0.0001	0.92 (0.86–0.95)
Spinal angle (°)	9.6 (4.4-14.8)	21.3 (17.7-27.4)	13.1 (9.2-16.3)	<0.0001	0.94 (0.89–0.97)

*Two-sided Wilcoxon signed-rank test for paired observations. *IQR*, interquartile range.

EOS radiographs confirmed that the experimental model induced anterior sagittal imbalance. Pelvic parameters (PI, PT, and SS) did not change significantly with brace application. In contrast, spinal alignment parameters changed significantly. Median C7ST increased from 1.2° (IQR, -3.2° to 1.3°) without the brace to 14.3° (IQR, 9.1° to 16.9°) with the brace ($p < 0.0001$). LL and TK also changed significantly, further confirming induction of anterior sagittal imbalance.

Relationship between radiographic and optoelectronic measurements

Optoelectronic measurements detected the induced sagittal imbalance in all participants. Median C7-T10-S1 angle decreased from 170.2° (IQR, 165.8°–172.9°) without the brace to 160.7° (IQR, 158.7°–164.1°) with the brace ($p < 0.0001$). Conversely, median spinal angle increased from 9.6° (IQR, 4.4°–14.8°) to 21.3° (IQR, 17.7°–27.4°) after brace application ($p < 0.0001$). EOS-derived C7ST showed moderate-to-strong correlations with all three dynamic parameters: C7-T10-S1 angle ($r_s = 0.62$), C7'S1' ($r_s = 0.70$), and spinal angle ($r_s = 0.69$) (Table 2).

Table 2. Relationship between EOS-derived C7 sagittal tilt and dynamic optoelectronic parameters.

Radiographic reference	Optoelectronic parameter	Spearman r_s	95% CI	p value
C7 sagittal tilt	C7–T10–S1 angle	0.62	0.47–0.72	<0.001
C7 sagittal tilt	C7'S1' parameter	0.70	0.56–0.80	<0.001
C7 sagittal tilt	Spinal angle	0.69	0.55–0.79	<0.001

Spearman correlation coefficients were estimated using the paired brace and no-brace observations. Confidence intervals were obtained using bias-corrected and accelerated bootstrap resampling at the participant level. *CI*, confidence interval; *EOS*, low-dose biplanar radiography.

Dynamic representation of sagittal alignment during gait

After synchronization and normalization of gait cycles, the C7-T10-S1 angle and spinal angle were visualized continuously throughout the gait cycle. Representative averaged curves are shown in Fig. 5.

Under the brace condition, curves were consistently shifted toward values indicating greater anterior trunk inclination. Cohort-level distribution envelopes showed similar patterns and illustrated between-participant variability. First-derivative curves also revealed differences in the rate of change in sagittal alignment. Overall, brace application altered dynamic alignment patterns in a manner consistent with experimentally induced anterior sagittal imbalance.

Diagnostic performance of optoelectronic parameters

The ability of radiographic and optoelectronic parameters to discriminate experimentally induced sagittal imbalance was evaluated using AUROC analysis (Fig. 6).

Among the optoelectronic parameters, the spinal angle showed the highest diagnostic performance (AUROC = 0.94), followed by C7'S1' (AUROC = 0.92) and the C7-T10-S1 angle (AUROC = 0.89). These values indicate excellent discrimination between the no-brace and brace conditions. Pelvic radiographic parameters showed poor discrimination, with AUROC values close to 0.50. Pairwise comparisons between AUROCs were not performed because the study was not powered for this analysis.

Discussion

Previous work established the feasibility of optoelectronic assessment of sagittal imbalance and demonstrated correlations with radiographic measurements [12]. The present study extends those findings by quantifying the diagnostic performance of three dynamic optoelectronic parameters using AUROC analysis and by developing a graphical approach for continuous characterization of sagittal alignment throughout the gait cycle.

Dynamic versus static assessment of sagittal alignment

Assessment of sagittal balance currently relies primarily on standing radiographs, including EOS imaging. These techniques accurately quantify spinopelvic alignment but provide only a static representation of posture [5, 11]. Gait requires continuous adaptation of the spine, pelvis, and lower limbs to maintain balance and forward progression, and compensatory mechanisms during walking may differ substantially from those observed during static standing [7–10]. The present findings show that dynamic optoelectronic parameters capture these postural adaptations while remaining associated with established radiographic parameters. Dynamic assessment should therefore be considered complementary to conventional imaging rather than a replacement for it. By providing continuous information throughout the gait cycle, optoelectronic analysis may support a more comprehensive evaluation of functional sagittal balance.

Validation of dynamic optoelectronic parameters

Interest in dynamic evaluation of spinal alignment and compensation mechanisms in patients with spinal deformity has increased in recent years [5, 7–11]. However, most studies have described kinematic patterns in specific pathological populations rather than validated dynamic sagittal alignment parameters against radiographic references. In the present study, EOS-derived C7ST correlated significantly with the C7-T10-S1 angle, C7'S1', and spinal angle. AUROC values approaching or exceeding 0.90 further indicated excellent discrimination of experimentally induced sagittal imbalance. These findings provide quantitative support for the validity of the proposed parameters as dynamic markers of sagittal alignment during gait.

Potential clinical applications

Dynamic assessment may complement static radiographs, as sagittal imbalance during walking may not be fully captured at rest [5, 10, 14–16]. The envelope defined by the 1st and 9th decile curves provides a simple visualization of alignment patterns and their variability throughout the gait cycle. Changes in amplitude, phase, periodicity, or envelope width may reveal impaired compensatory mechanisms. This approach could be particularly relevant in ankylosing spondylitis, where spinal rigidity and fixed kyphosis may produce an attenuated or irregular dynamic signal [17]. It may also help characterize functional adaptation and treatment response in adult spinal deformity and adolescent idiopathic scoliosis [7, 8]. Validation in clinical populations is required before individual application.

Graphical representation of sagittal alignment during gait

This study also introduces an intuitive method for visualizing sagittal alignment during gait. Unlike a single summary value, the 1st–9th decile envelope displays curve shape, variability, amplitude, and timing throughout the gait cycle. Previous work demonstrated the feasibility of detecting sagittal imbalance using motion capture [12]; the present study further showed good-to-excellent discrimination for the spinal angle, C7'S1', and C7-T10-S1 angle between the no-brace and experimentally induced imbalance conditions. This dynamic representation could therefore provide a clinically interpretable functional marker of sagittal imbalance. Future studies should automate curve analysis and validate disease-specific patterns in clinical cohorts under real-life walking conditions.

Limitations

Several limitations should be acknowledged. First, the study included only healthy young male volunteers, limiting generalizability to women and pathological populations. Second, sagittal imbalance was induced using a kyphosing brace and therefore did not reproduce the complexity of clinical spinal deformity. The purpose of this model was to create a controlled sagittal perturbation for validation rather than to mimic a specific disorder. Third, the sample size was modest, although each participant completed multiple trials under both conditions. The study was not powered for pairwise comparisons between AUROCs. Finally, the parameters were validated against radiographic alignment measurements but not against clinical outcomes. Further studies are needed to establish their clinical relevance and responsiveness to treatment.

Conclusion

Dynamic optoelectronic analysis provides a feasible method for assessing sagittal alignment during gait. The proposed parameters showed moderate-to-strong correlations with conventional EOS measurements and excellent ability to detect experimentally induced sagittal imbalance. By complementing static radiographic evaluation with continuous functional assessment, optoelectronic analysis may contribute to a more comprehensive understanding of sagittal balance in patients with spinal deformity.

Declarations

Conflict of interest : The authors declare the following relationships reported in the French public transparency register: M. Ould-Slimane (€38,000). The remaining authors declare that they have no competing interests. These declarations are provided irrespective of any direct relationship with the present study.

Funding : This research did not receive any specific grant from funding agencies in the public, commercial, or not-for-profit sectors.

Ethics approval : Institutional Review Board approval was obtained before study initiation.

Informed consent: Informed consent was obtained from all patients and/or their legal guardians according to institutional requirements.

Data availability : The datasets generated and/or analysed during the current study are available from the corresponding author upon reasonable request.

Declaration of generative AI and AI-assisted technologies in the writing process : During the preparation of this manuscript, the authors used ChatGPT (OpenAI) to improve the language and readability of the text. The authors carefully reviewed and edited the generated content and take full responsibility for the content of the publication.

References

1. Iyer, S. et al. Sagittal spinal alignment in adult spinal deformity: an overview of current concepts and a critical analysis review. *JBJS Rev.* **6,** e2 (2018).
2. Berthonnaud, E., Dimnet, J., Roussouly, P. & Labelle, H. Analysis of the sagittal balance of the spine and pelvis using shape and orientation parameters. *J. Spinal Disord. Tech.* **18,** 40-47 (2005).
3. Barrey, C., Roussouly, P., Le Huec, J. C., D'Acunzi, G. & Perrin, G. Compensatory mechanisms contributing to keep the sagittal balance of the spine. *Eur. Spine J.* **22,** S834-S841 (2013).
4. Hasegawa, K. et al. Compensation for standing posture by whole-body sagittal alignment in relation to health-related quality of life. *Bone Joint J.* **102-B,** 1359-1367 (2020).
5. Diebo, B. G. et al. From static spinal alignment to dynamic body balance: utilizing motion analysis in spinal deformity surgery. *JBJS Rev.* **6,** e3 (2018).
6. Glassman, S. D., Berven, S., Bridwell, K., Horton, W. & Dimar, J. R. Correlation of radiographic parameters and clinical symptoms in adult scoliosis. *Spine (Phila. Pa. 1976)* **30,** 682-688 (2005).
7. Pesenti, S. et al. Correlations linking static quantitative gait analysis parameters to radiographic parameters in adolescent idiopathic scoliosis. *Orthop. Traumatol. Surg. Res.* **105,** 541-545 (2019).
8. Pesenti, S. et al. Does static trunk motion analysis reflect its true position during daily activities in adolescent idiopathic scoliosis? *Orthop. Traumatol. Surg. Res.* **106,** 1251-1256 (2020).
9. Blondel, B. et al. Postural spinal balance defined by net intersegmental moments: results of a biomechanical approach and experimental errors measurement. *World J. Orthop.* **6,** 983-990 (2015).
10. Severijns, P. et al. Dynamic sagittal alignment and compensation strategies in adult spinal deformity during walking. *Spine J.* **21,** 1059-1071 (2021).
11. Simon, A. L., Ilharreborde, B., Souchet, P. & Kaufman, K. R. Dynamic balance assessment during gait in spinal pathologies: a literature review. *Orthop. Traumatol. Surg. Res.* **101,** 235-246 (2015).
12. Ould-Slimane, M. et al. Noninvasive optoelectronic assessment of induced sagittal imbalance using the Vicon system. *World Neurosurg.* **102,** 425-433 (2017).
13. Efron, B. & Narasimhan, B. The automatic construction of bootstrap confidence intervals. *J. Comput. Graph. Stat.* **29,** 608-619 (2020).

14. Smith, J. S. et al. Clinical and radiographic evaluation of the adult spinal deformity patient. *Neurosurg. Clin. N. Am.* **24,** 143-156 (2013).
15. Le Huec, J. C. & Roussouly, P. Sagittal spino-pelvic balance is a crucial analysis for normal and degenerative spine. *Eur. Spine J.* **20,** 556-557 (2011).
16. Lafage, V., Schwab, F., Patel, A., Hawkinson, N. & Farcy, J. P. Pelvic tilt and truncal inclination: two key radiographic parameters in the setting of adults with spinal deformity. *Spine (Phila. Pa. 1976)* **34,** E599-E606 (2009).
17. Song, D., Zheng, G., Wang, T., Qi, D. & Wang, Y. Increasing pelvic incidence is associated with more global sagittal imbalance in ankylosing spondylitis with thoracolumbar kyphosis: an observational retrospective study of 94 cases. *BMC Musculoskelet. Disord.* **21,** 192 (2020).

Figures

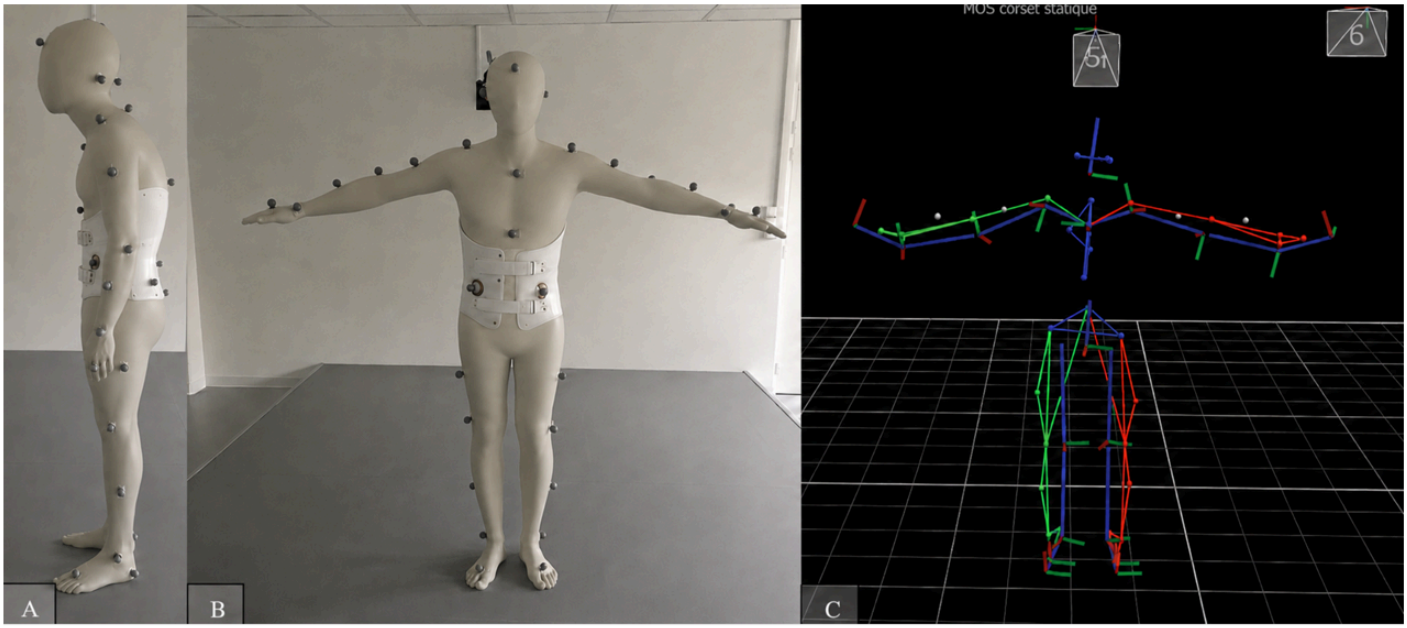


Figure 1

Experimental setup for optoelectronic assessment of sagittal alignment.

(**A :** Lateral view illustrating the experimentally induced anterior sagittal imbalance produced by the brace ; **B :** Frontal view of the participant wearing the custom-made kyphosing brace with the complete set of 38 reflective markers positioned according to the standardized Vicon protocol ; **C :** Three-dimensional skeletal reconstruction generated by the Vicon® motion capture system from the reflective markers).

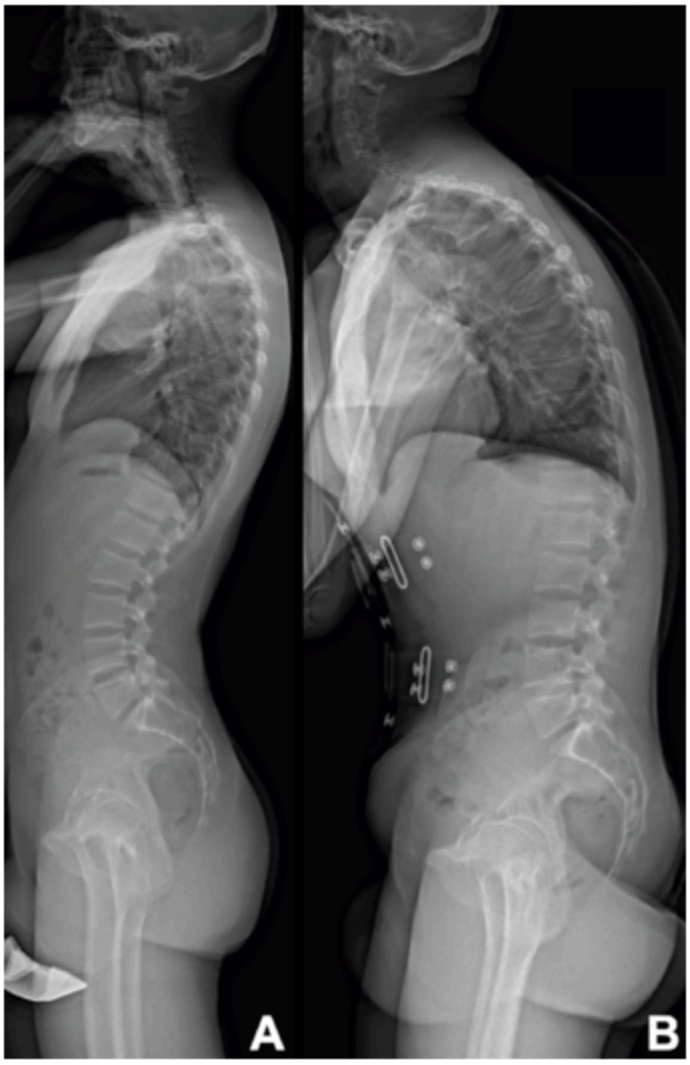


Figure 2

EOS validation of experimentally induced sagittal imbalance (A : without brace ; B : with brace).

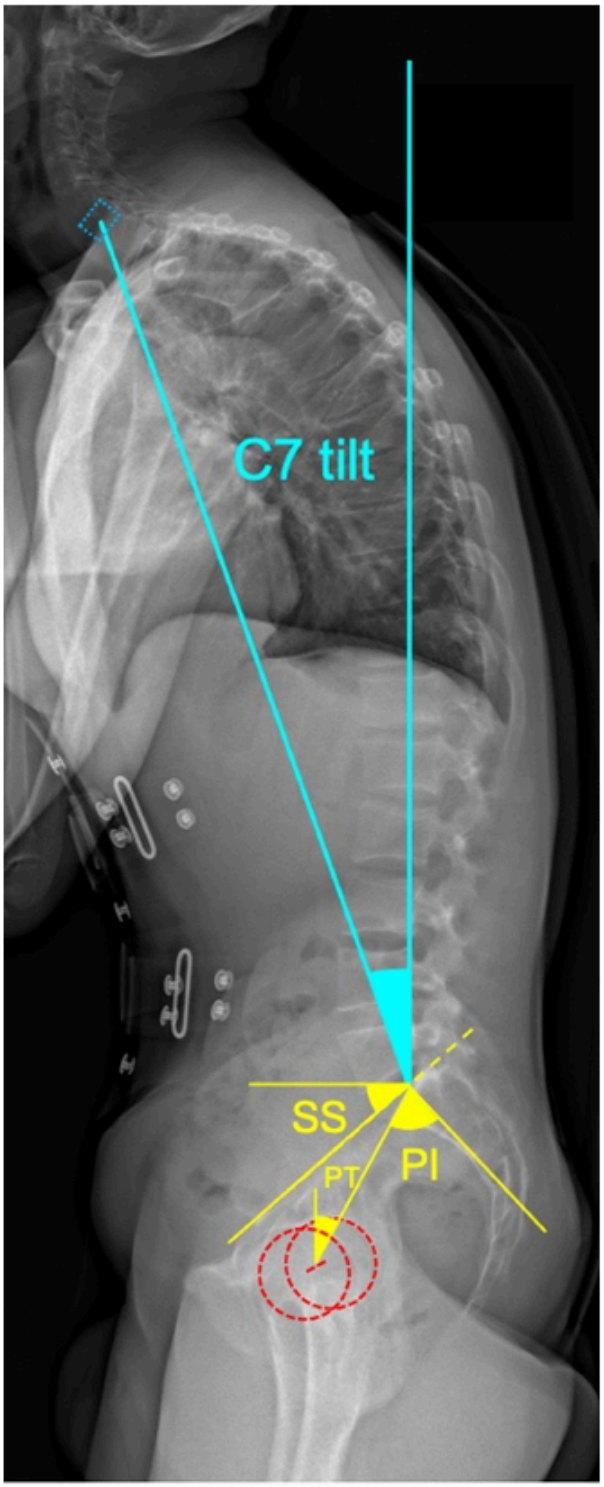


Figure 3

Radiographic sagittal balance parameters measured on EOS lateral radiographs.

(C7 tilt: C7 Sagittal Tilt; PI: Pelvic Incidence; SS: Sacral Slope; PT: Pelvic Tilt)

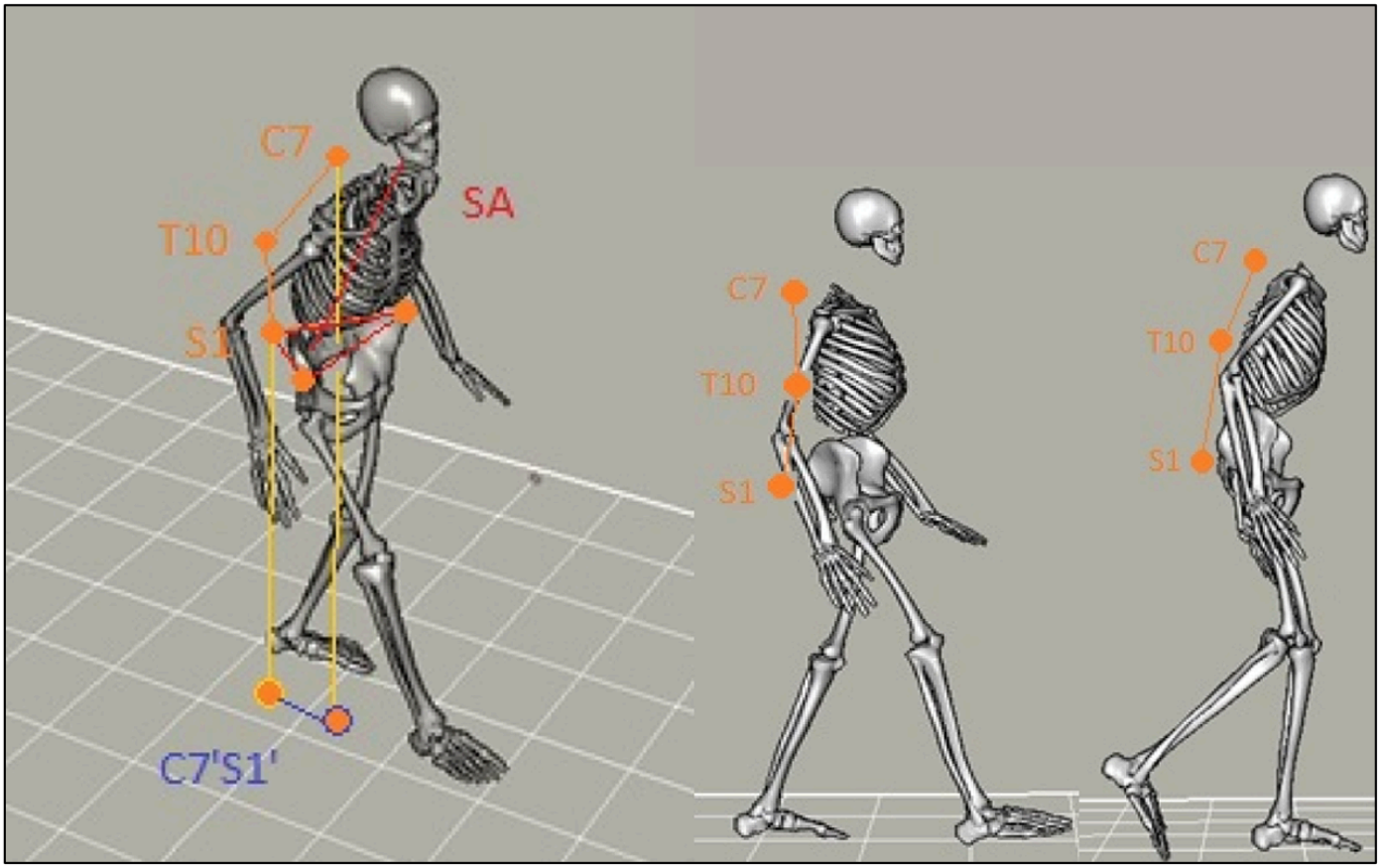


Figure 4

Definition of the dynamic optoelectronic parameters.

(C7-T10-S1 angle, SA: spinal angle, C7'S1'distance)

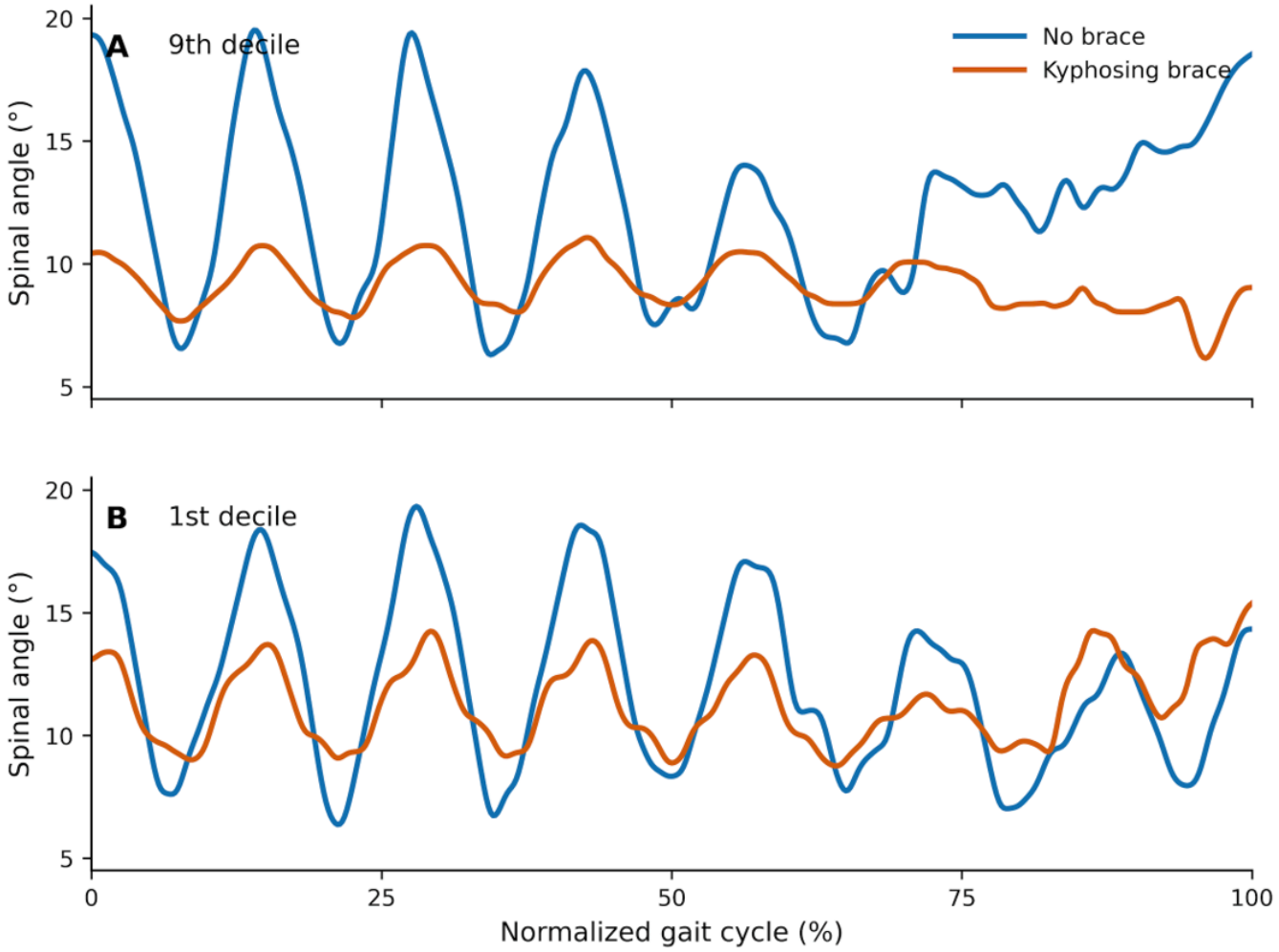


Figure 5

Dynamic sagittal alignment during gait.

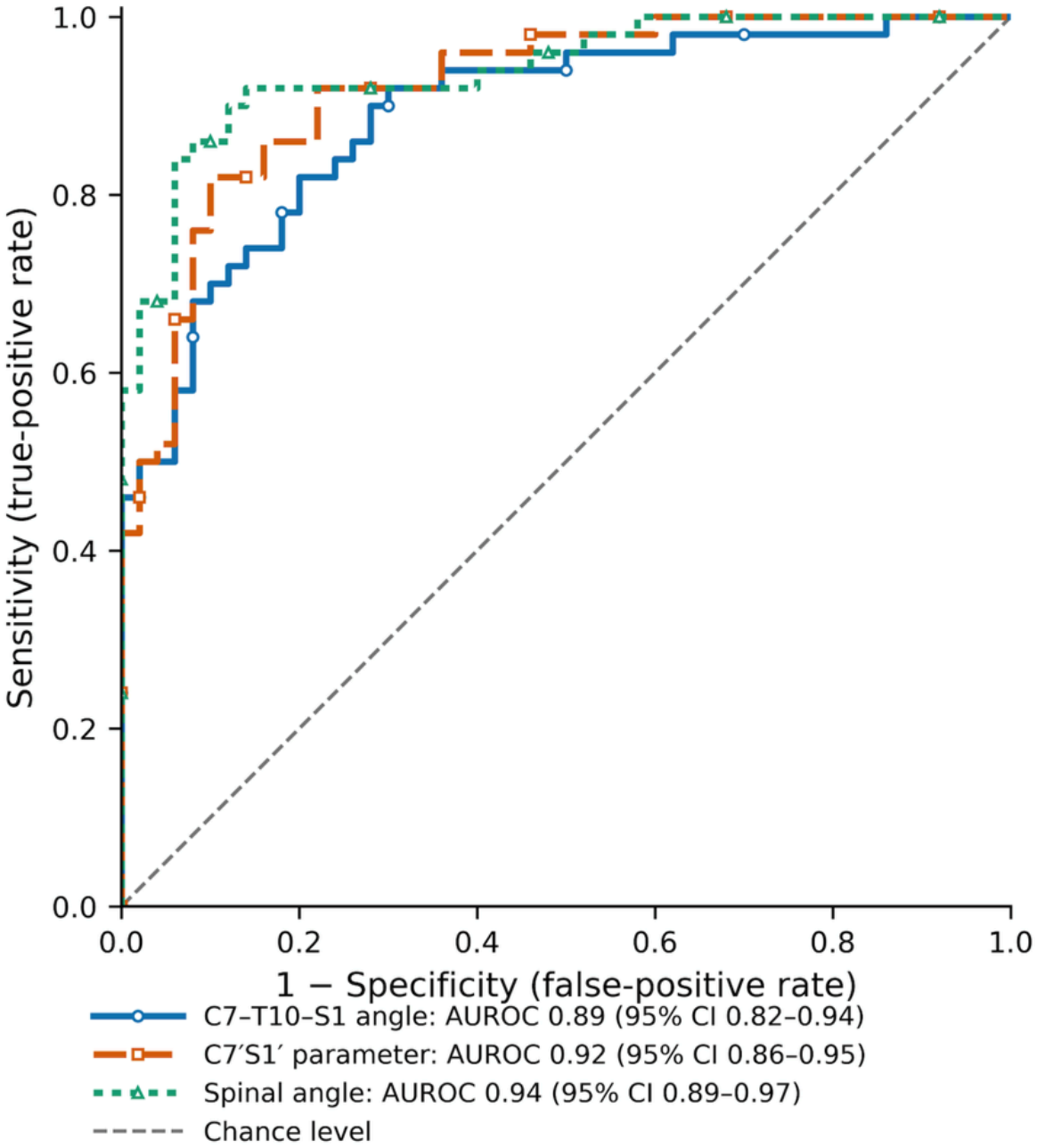


Figure 6

Diagnostic performance of dynamic optoelectronic parameters for detecting sagittal imbalance.